[AMERICAN JOURNAL OF SCIENCE, VOL. 288-A, 1988, P. 45–74]

SILICATE-SULFIDE-OXIDE-FLUID REACTIONS IN GRANULITE-GRADE PELITIC ROCKS, CENTRAL MASSACHUSETTS

ROBERT J. TRACY* and PETER ROBINSON**

ABSTRACT. Sulfidic, graphitic pelitic schists are abundant in central Massachusetts at metamorphic grades as high as the lower part of the granulite facies. They consist of two rock types, those with minor pyrrhotite and graphite along with typical silicate-oxide mineral assemblages and those containing unusually high modal sulfide and graphite with very magnesian silicate-oxide assemblages. The most sulfur-rich of this latter group may even contain primary pyrite at metamorphic grade far above its more common stability limit. The typical mineral assemblage for these highly sulfidic granulite grade pelites is quartz–Kfeldspar–plagioclase–biotite–cordierite–sillimanite–rutile–pyrrhotite–graphite ± pyrite. The range in Fe/(Fe + Mg) for biotite is from 0.41 to <0.01, and the range for cordierite is from 0.27 to <0.01. Although they are in rocks saturated with rutile, the most magnesian biotites show very low TiO_2 for this high grade and higher F contents than other biotites from this terrane. Three very Mg-rich cordierites that coexist with pyrrhotite + pyrite contain sulfur assumed to be in the form of H_2S replacing H_2O in the structural channels due to high X_{H_2S} in metamorphic fluid. This is the first known occurrence of sulfur-bearing cordierite. Sulfur isotopic data for sulfides in several samples indicate the light sulfur ($\delta^{34}S$ of −25 to −30) that is typical of bacterially-fixed sulfide in sediments deposited in euxinic or anoxic conditions. We propose that the formation of the sulfidic schist protoliths occurs at the sedimentary or diagenetic stage through reaction of bacterially produced H_2S with detrital minerals to produce authigenic pyrite.

The topology of high-grade metamorphic sulfide–silicate–oxide reactions suggests that very magnesian assemblages were produced through sulfidation of ferromagnesian silicates and Fe-Ti oxides in the presence of H_2S-rich metamorphic fluid, with conversion of pyrite to pyrrhotite occurring as a byproduct of the reactions. Fe is therefore progressively and effectively removed from the reactive bulk composition of the rock and sequestered in pyrrhotite. The relatively rare rocks in which pyrite was still present at metamorphic temperatures exceeding 700°C represent protoliths that had such high S/Fe ratios (>1.0) that complete removal of Fe from the silicate-oxide assemblage could occur before all pyrite was converted. The phase equilibria in the Massachusetts samples strongly suggest isochemical metamorphism with only minor loss of initially solid-state components C and S through incorporation into a fluid phase and no involvement of significant volumes of externally derived fluid. Fluid composition calculations indicate very high H_2S in fluids in two-

* Department of Geological Sciences, Virginia Polytechnic Institute and State University, Blacksburg, Virginia 24061

** Department of Geology and Geography, University of Massachusetts, Amherst, Massachusetts 01003

sulfide rocks (X_{H_2O} = 0.35; X_{H_2S} = 0.51; X_{CO_2} = 0.13; X_{CH_4} = 0.01), whereas fluid in a pyrrhotite-only sample with Fe-bearing silicates was quite different and much lower in H_2S (X_{H_2O} = 0.79; X_{H_2S} = 0.04; X_{CO_2} = 0.05; X_{CH_4} = 0.11).

INTRODUCTION

The iron sulfide minerals pyrite and pyrrhotite are common constituents of metamorphic rocks and typically coexist with graphite in chemically reduced pelitic schists. Such sulfidic, graphitic schists are relatively abundant in New England. There they fall into two general categories based on mineral assemblages as a reflection of bulk chemistry. The first group are schists that display relatively low-variance assemblages and that have a low S content in the bulk composition. They are characterized by Fe-bearing silicates and oxides and by low modal abundances of sulfides. Typically the only difference between these rocks and adjacent non-sulfidic schists is a shift in the proportions of ferromagnesian minerals. For example, a reduction in the modal amount of more iron-rich phases such as garnet or ilmenite results from the incorporation of reduced iron into pyrite or pyrrhotite. The second group is characterized by sulfur contents high enough to cause the disappearance of one or more iron-rich oxide or silicate phases. This results in atypical and unusually magnesian silicate-oxide assemblages of higher variance than those of group one. A subcategory of group two includes sulfidic schists of such high sulfur content that most or all of the iron in the rock is locked up in iron sulfides. These rocks are considerably rarer than the less sulfidic schists, are invariably graphitic, and have probably resulted from the metamorphism of fine-grained sediments deposited in anoxic or even euxinic conditions.

It has been clearly established that diagenetic and metamorphic iron sulfides react with each other and with silicates and oxides during metamorphism (Froese, 1969; Thompson, 1972; Guidotti, Cheney, and Conatore, 1975; Guidotti, Cheney, and Henry, 1976; Robinson and Tracy, 1977; Ferry, 1981; Mohr and Newton, 1983). Even though sulfides may be volumetrically minor in most sulfidic metamorphic rocks, sulfide-silicate and sulfide-oxide reactions generally can be shown to have had observable to pronounced effects on the silicate-oxide phase equilibria. Froese (1971) has elegantly shown the thermodynamic and graphical techniques for dealing with sulfidation-oxidation reactions involving several ferromagnesian silicates. Although Froese did not deal explicitly with the question of the interdependence of sulfidation-oxidation reactions and mixed-volatile equilibria in metamorphic rocks, a number of later reports have discussed this point (Robinson and Tracy, 1977; Nesbitt and Kelly, 1980; Ferry, 1981; Mohr and Newton, 1983).

Several topics will be discussed in some detail in this paper, including the petrology of a group of high-grade sulfidic schists from central New England, the sedimentary geochemistry of sulfidic schist protoliths, and the general implications of sulfide–silicate–oxide reac-

tions for phase relations and fluid compositions in pelitic schists. The previous studies of metamorphosed sulfidic rocks cited above have examined considerably lower grade rocks than those we report on here, typically not higher than about staurolite grade. The sulfidic schists from Massachusetts reached granulite grade and display notable features not observed in the studies at lower grade. It is our hope that the discussion below will emphasize the potential influence of volumetrically minor phases on the phase relations of the major phases and stimulate more complete and precise petrographic work by those examining sulfidic rocks.

GEOLOGIC SETTING OF SULFIDIC SCHISTS IN MASSACHUSETTS

Sulfidic, graphitic schists abound in central Massachusetts, including the well known pyrrhotite schists of the Middle Ordovician Partridge Formation in which minor sulfide and graphite occur in mineral assemblages typical for pelitic schists at each appropriate metamorphic grade. The Partridge also contains minor volumes of rock types with slightly Mg-enriched assemblages, especially at higher grade. There is also the more sulfidic "White Schist Member" of the Paxton Formation, first defined by Field (1975), which extends across the state. Regional studies now suggest that it is certainly correlative with the Silurian Smalls Falls Formation of northwestern Maine where Guidotti, Cheney, and Conatore (1975), and Guidotti, Cheney, and Henry (1976) have done detailed petrologic studies. It is characteristic of these highly sulfidic and graphitic rock types, both at lower metamorphic grade in Maine (chlorite) and at higher grade in Massachusetts (granulite), that extremely magnesian assemblages were commonly produced during metamorphism due to effective removal of iron from the bulk composition by fractionation into sulfide, thereby making the iron inaccessible to the reacting silicates and oxides. In fact, as Guidotti, Cheney, and Conatore (1975) noted, this phenomenon makes accessible the highly magnesian part of pelitic schist composition space, so that the topology of metamorphic mineral assemblages for these unusual compositions may be documented.

Highly sulfidic samples of the "White Schist Member" have been collected at metamorphic grades ranging from sillimanite–muscovite–Kspar (zone IV of Tracy, 1978, and Robinson and others, 1982) to sillimanite–Kspar–garnet–cordierite (zone VI). Sample locations are shown in figure 1 on a modified geologic-metamorphic map of central Massachusetts. Metamorphic pressures for this area have been estimated as 6 to 6.5 kb, and metamorphic temperatures based largely on garnet-biotite thermometry range from about 650°C for zone IV to 720°C for zone VI (Tracy, Robinson, and Thompson, 1976; Robinson and others, 1982). The detailed petrology of relatively few samples is discussed in this paper, largely because of the extreme difficulty of collecting fresh enough material for analytical work. The highly sulfidic schists are subject to very rapid chemical weathering through leaching and oxida-

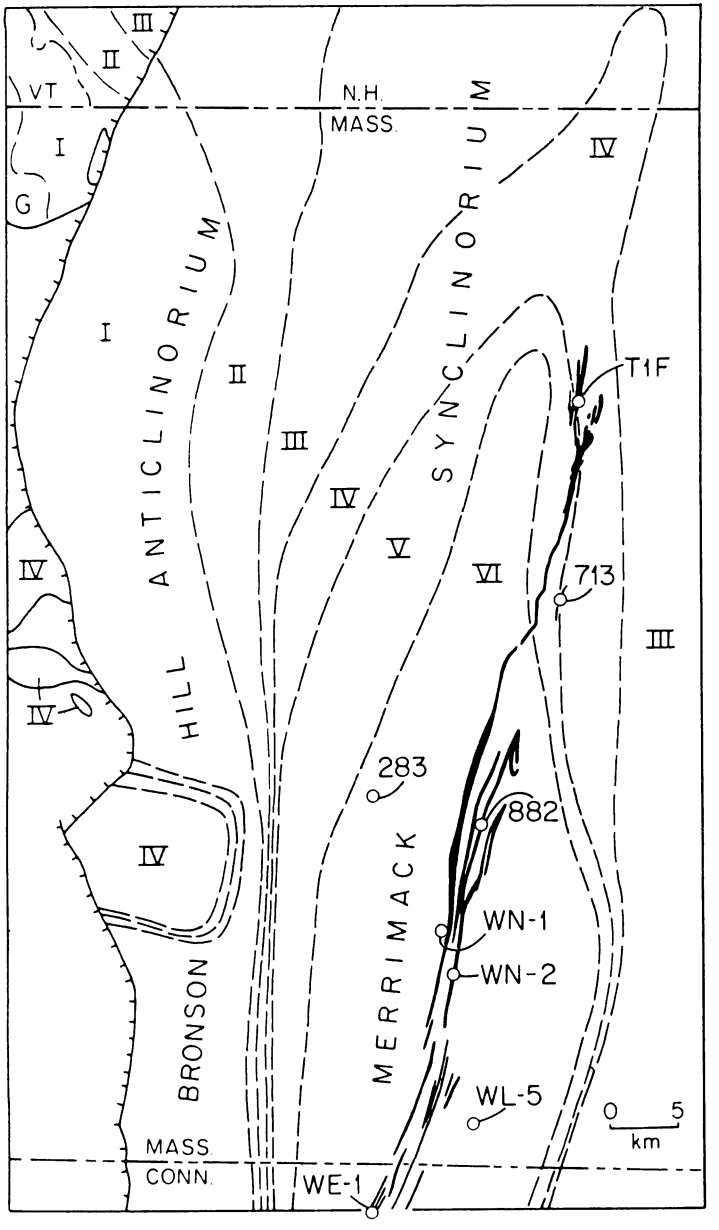

Fig. 1. Map of Acadian prograde metamorphic zones in central Massachusetts and adjacent parts of Vermont, New Hampshire, and Connecticut, showing locations of sulfidic schist samples analyzed for this study. Solid black indicates distribution of sulfidic magnesian biotite-cordierite schist of the Paxton Formation (Zen and others, 1983) that is lithically correlated with the mid-Silurian Smalls Falls Formation of Maine. Hachured line indicates Mesozoic Connecticut Valley border fault with hachures on the downthrown side. Unlabelled areas are Mesozoic sedimentary and volcanic rocks. G = garnet zone, I = staurolite-kyanite zone, II = staurolite-sillimanite zone, III = sillimanite-muscovite zone, IV = sillimanite-muscovite-orthoclase zone, V = sillimanite-orthoclase zone, and VI = sillimanite-orthoclase-garnet-cordierite zone.

tion of pyrrhotite into sulfuric acid. Consequently, collection from natural outcrops is rarely possible, and only very recent man-made exposures can be profitably sampled.

The metamorphic and tectonic history of central Massachusetts has been described in detail by Robinson and others (1982), Robinson, Field, and Tucker (1982), and Robinson and others (1986). Briefly, the area from which the "White Schist Member" samples were collected lies at the western edge of the Merrimack synclinorium, a package of Lower Silurian through Lower Devonian metamorphosed sedimentary and volcanic rocks deposited in a rapidly eastward-thickening depositional basin. The area was intensely metamorphosed and deformed in the Devonian Acadian Orogeny and now lies near the center of the so-called eastern Acadian metamorphic high (Robinson, 1983).

PETROGRAPHY AND MINERAL CHEMISTRY

Principal constituent minerals of the "White Schist Member" sulfidic, graphitic schists include quartz, K-feldspar, sillimanite (commonly pseudomorphic after andalusite), cordierite, biotite, graphite, and pyrrhotite. In addition, ilmenite, rutile, pyrite, and muscovite may be present. Mineral assemblages for the samples that have undergone detailed examination are given in table 1. Note that the most common silicate assemblage is qtz–plag–Ksp–sill–bio–cord, with only one of the analyzed samples containing muscovite in addition (T1F). Sample 283 is a typical example of the high-grade pyrrhotitic schist of the Silurian Rangeley Formation in which sulfide is modally minor and more Fe-rich minerals such as garnet and ilmenite are possible. Three samples listed in table 1 contain pyrite, and it should be emphasized that this is primary metamorphic pyrite, despite the high metamorphic grade. The persistence of pyrite in these rocks far beyond its typical upper stability will be discussed below.

Total sulfide mineral contents of the samples in table 1 (except for 283) range from 10 to about 30 modal percent. The most sulfide-rich samples resemble ores in hand specimen. Sample 283 contains minor (less than 5 modal percent) pyrrhotite. Most of the samples are gneissose rather than schistose, because they are predominantly quartzofeldspathic. Modal biotite is typically less than 10 percent and is lowest in the samples with the most magnesian compositions. A common feature of the sulfidic rocks is the occurrence of cordierite as large (up to 1 cm) rounded black knots in which numerous sulfide inclusions may be seen. Thin-section observation shows that these cordierites are typically inclusion-rich, with quartz, rutile, and graphite in addition to sulfide. Many samples typically have moderate to high graphite contents, and some samples leave black smears on hands or paper. A coarse-grained pegmatoid quartz-Kfeldspar segregation at location WN-2, possibly an anatectic melt, contains graphite flakes up to several centimeters across that may have recrystallized and coarsened in the presence of melt or C–O–H (–S) fluid. Much of the sillimanite in the samples occurs in peculiar columnar aggregates which resemble andalusite crystals in their

TABLE 1

Mineral assemblages in sulfidic schists

	882E	T-1F	882Y	WN-2A	WN-2B	WE-1	713	WL-5A	WN-1A	WN-1B	283
Quartz	x	x	x	x	x	x	x	x	x	x	x
Plagioclase[2]	36	37	36	29	45	36	42	38	43	36	19
Kspar	x	x	x	x	x	x	x	x	x	x	x
Sillimanite	x	x	x	x	x	x	x	x	x	x	x
Muscovite		x									
Biotite	x	x	x	x	x	x	x	x	x	x	x
Cordierite	x	x	x	x	x	x	x	x	x	x	x
Garnet											x
Ilmenite									x	x	x
Rutile	x	x	x	x	x	x	x	x			
Pyrrhotite	x	x	x	x	x	x	x	x	x	x	x
Pyrite	x	x	x								
Graphite	x	x	x	x	x	x	x	x	x	x	x

[2]Anorthite content.

morphology. In this same terrane, Rosenfeld (1969) and Tracy and Robinson (1980) have reported sillimanite pseudomorphs after andalusite in other pelitic rock types.

Electron microprobe analyses of biotites and cordierites have been performed on two microprobes: an ETEC Autoprobe at the University of Massachusetts, Amherst, and an ARL SEMQ at Virginia Polytechnic Institute and State University Analyses were done using natural and synthetic oxide and silicate standards; data reduction was done according to the method of Bence and Albee (1968) using correction factors from Albee and Ray (1971).

Analyzed biotites (table 2) range widely in composition from Fe/(Fe + Mg) of nearly 0.5 to 0.01. Biotites with Fe-Mg ratios above about 0.2 have brown to reddish-brown color, and the typical thin-section appearance of pelitic biotites. The more magnesian biotites, however, are distinctly pale in color or even colorless (882Y, 882E, T1F). These most magnesian biotites are also very low in TiO_2 for such high-grade biotites, despite being saturated with TiO_2 through their coexistence with rutile. Guidotti, Cheney, and Guggenheim (1977) noted similar effects in biotites from Maine, and Guidotti (1984) presented a crystal-chemical explanation. Table 2 also shows that the most magnesian biotites (882Y, 882E, and T1F) are notably richer in fluorine than all but one of the more Fe-rich biotites. This difference may indicate consistent compositional contrasts in fluids between the most sulfidic and the other samples, but it is more likely due to the previously observed effect that F seems to occur preferentially in more magnesian biotites (Guidotti, 1984, p. 427–430). Munoz and Ludington (1974) have suggested that this effect is due to preferential bonding of F with Mg in biotites. Although the three most magnesian biotites have notably higher F than all but one of the others, the data of table 2 doesn't indicate any consistent decrease in F content with increasing Fe. In any case, it is likely that the approx 20 percent of fluor-biotite component in the three Mg-rich biotites may have some effect on the stability of this mineral.

Table 3 lists microprobe analyses of cordierites in the sulfidic schists. The cordierites, like the biotites, show a wide range in composition. Sample 283 has relatively Fe-rich cordierite typical of that in garnet-bearing rocks from central New England, whereas 882Y and 882E have essentially pure magnesium cordierites. A notable peculiarity of the chemistry of the cordierites in 882Y, 882E, and T1F (all containing two sulfides) is that they all appear to contain significant sulfur. Sulfur was first detected by EDS in these samples and then was analyzed with WDS. It was looked for, but not detected, in any of the other samples. In table 3 the sulfur is reported as H_2S, because it is presumed to occur in this reduced form replacing H_2O in the structural channels in cordierite, but this has not yet been proved by spectroscopic or other tests. The sulfur is certainly not present as finely disseminated or submicroscopic iron sulfides, because little or no iron was detected in

TABLE 2

Microprobe analyses of biotites

	882E	T-1F	882Y	WN-2A	WN-2B	WE-1	713	WL-5A	WN-1A	WN-1B	283
SiO_2	40.96	39.77	40.63	38.57	37.58	38.57	38.50	37.40	36.79	36.28	35.48
TiO_2	1.21	1.09	1.28	2.96	3.30	3.55	2.17	3.53	3.45	4.13	4.21
Al_2O_3	19.95	19.47	19.04	19.51	19.17	18.64	19.48	18.11	17.92	17.30	18.46
FeO	0.02	2.16	0.71	8.11	8.46	8.88	8.97	12.14	14.63	15.77	16.78
MnO	0.03	0.36	0.13	0.49	0.71	0.34	0.13	0.26	0.11	0.07	0.04
MgO	22.75	21.62	22.92	18.59	17.13	17.37	16.70	15.41	14.98	12.79	11.88
Na_2O	0.07	0.06	0.06	0.07	0.08	0.10	0.22	0.13	0.12	0.19	0.12
K_2O	10.02	9.90	10.17	10.03	9.79	9.99	9.27	9.85	9.99	10.05	9.82
F	0.91	0.65	1.15	0.23	0.20	0.23	0.50	0.46	0.69	0.53	0.35
Cl	0	0	0.01	0.01	0.02	0	0	0	0	0.01	0
	95.54	94.81	95.61	98.46	96.34	97.57	95.73	97.10	98.39	96.89	96.99
Formulas based on 11 (O + F + Cl)											
Si	2.824	2.798	2.809	2.692	2.690	2.711	2.761	2.702	2.668	2.691	2.634
Al	1.176	1.202	1.191	1.308	1.310	1.289	1.239	1.298	1.332	1.309	1.366
	4.000	4.000	4.000	4.000	4.000	4.000	4.000	4.000	4.000	4.000	4.000
Al	.445	.413	.361	.296	.308	.255	.408	.244	.198	.203	.250
Ti	.062	.057	.081	.153	.176	.213	.116	.192	.187	.230	.235
Fe	.001	.127	.041	.473	.506	.522	.538	.733	.885	.977	1.042
Mn	.002	.021	.007	.028	.042	.020	.007	.016	.006	.004	.002
Mg	2.338	2.267	2.361	1.934	1.829	1.820	1.786	1.659	1.619	1.414	1.315
	2.848	2.885	2.851	2.884	2.861	2.830	2.855	2.844	2.895	2.828	2.844
Na	.010	.009	.008	.008	.010	.014	.013	.018	.015	.027	.017
K	.882	.889	.897	.891	.893	.896	.848	.908	.923	.953	.930
	.892	.898	.905	.899	.903	.910	.861	.926	.938	.980	.947
F	.199	.144	.251	.052	.045	.051	.118	.105	.160	.121	.095
Cl	0	.002	0	.002	.003	0	0	0	0	.002	0
Fe/(Fe + Mg)	0	.053	.017	.197	.217	.223	.232	.306	.353	.409	.442

TABLE 3

Microprobe analyses of cordierites

	882E	T-1F	882Y	WN-2A	WN-2B	WE-1	713	WL-5A	WN-1A	WN-1B	283
SiO_2	49.87	50.55	49.86	49.57	48.93	50.25	49.04	49.78	49.60	48.97	48.18
Al_2O_3	34.11	34.16	34.08	33.98	33.29	34.49	33.41	34.42	34.04	32.46	33.92
FeO	0.01	0.06	0.14	2.51	2.64	3.11	3.10	4.38	5.66	6.61	5.99
MnO	0.01	0.06	0.04	0.69	0.83	0.46	0.34	0.50	0.17	0.18	0.17
MgO	13.68	13.62	13.64	12.24	11.71	11.92	11.30	11.04	10.61	9.98	10.06
Na_2O	0.06	0.10	0.09	0.16	0.11	0.09	0.22	0.11	0.18	0.12	0.18
H_2S	1.49	0.93	1.02	0	0	0	0	0	0	0	0
	99.23	99.48	98.88	99.15	97.51	100.32	97.41	100.23	100.27	98.32	98.50
Formulas based on 18 oxygens											
Si	4.975	4.993	4.972	4.945	4.967	4.953	4.982	4.950	4.949	5.008	4.905
Al	4.010	3.977	4.005	3.996	3.983	4.006	4.003	4.034	4.003	3.914	4.073
	8.985	8.970	8.975	8.941	8.983	8.959	8.985	8.984	8.952	8.922	8.978
Fe	.001	.005	.011	.208	.223	.257	.263	.363	.471	.566	.510
Mn	.001	.005	.003	.055	.068	.038	.029	.042	.011	.016	.014
Mg	2.034	2.006	2.027	1.818	1.770	1.751	1.712	1.636	1.578	1.520	1.527
Na	.011	.021	.017	.029	.021	.018	.043	.020	.032	.023	.034
H_2S	.256	.160	.175	0	0	0	0	0	0	0	0
Fe/Fe+Mg)	.001	.002	.005	.103	.112	.128	.133	.182	.230	.271	.250

these analyses. A search of the literature has turned up no other reports of sulfur in cordierite.

It is not coincidental that the only sulfur-bearing cordierites in this study are those from rocks containing primary metamorphic pyrite as well as pyrrhotite. The coexistence of pyrite plus pyrrhotite, especially at the high T and P of these rocks (700°C, 6000 bars) buffers a very high fugacity of S_2 ($\log f_{S_2} = 0.3$) (Toulmin and Barton, 1964). This, together with low calculated oxygen fugacity, results in calculated fluid compositions in which H_2S is a major constituent. Lower sulfur activities in pyrrhotite-only samples lead to calculated fluids with an order of magnitude less H_2S. Apparently, fluids rich in H_2S can introduce this species into the cordierite structure, with unknown effects on cordierite stability. Presumably there is some threshold value of H_2S fugacity that causes this effect, but the data from this study are not sufficient to define this threshold except to say that it probably falls at or below 50 mole percent H_2S at 700°C and 6 kb. It was noted above that relatively high F in biotites from the most magnesian samples could stabilize this phase in dehydration reactions (Valley and others, 1982) such as those to be discussed below. By similar argument, the presence of H_2S in cordierite could enhance the stability of this mineral in highly sulfidic rocks.

SEDIMENTARY ORIGIN OF SULFIDIC, GRAPHITIC SCHISTS

When most petrologists are confronted with highly sulfidic and graphitic sedimentary or metamorphic rocks, they immediately consider the depositional origins of these rocks as ancient analogues of modern euxinic depositional environments, the classic being the Black Sea. In fact, only part of the Black Sea contains euxinic bottom conditions (Rozanov, Volkov, and Yagodinskaya, 1974) defined geochemically as conditions where bottom seawater is not only anoxic but actually contains dissolved H_2S (Berner, 1981). According to Berner's suggested classification, the preferred term for ancient environments would be "anoxic," and this usage will be followed here.

Ferry (1981) raised the issue of the state in which iron and sulfur occurred in post-diagenetic shales, arguing that all the iron in such rocks (the precursors to sulfidic schists) occurred in sedimentary sulfide, typically pyrite. This point is crucial to interpretations of metamorphic pyrite-pyrrhotite reactions, because conversion of pyrite to pyrrhotite with increasing temperature requires either the availability of iron and a fixed amount of sulfur (producing two moles of pyrrhotite for every mole of pyrite) or the loss of sulfur (producing one mole of pyrrhotite for every mole of pyrite). A third possibility is that sulfur introduced into the rocks in H_2S-bearing metamorphic fluid could react with iron-bearing oxides or silicates to produce pyrite (at lower temperature) or pyrrhotite (at higher T). Production of pyrrhotite in this manner would render meaningless the molar proportion of pyrrhotite as a discriminator between the fixed-iron and fixed-sulfur scenarios.

Ferry based his interpretations of mineral assemblages and compositions on the basic assumption that all iron in the sedimentary protoliths

was sulfide iron. This assumption may apply to the calcareous shales from Maine that he studied but does not appear to apply to typical deep-water shales. Berner (1984) noted that only rarely, and typically only in highly calcareous sediments, did the total amount of iron control the amount of sedimentary sulfide produced in a shale. A much more common control is the *reactivity* of iron in the sediment. Unreactive iron tied up in detrital silicates and oxides is generally not accessible in the sedimentary sulfide-forming process except in certain highly euxinic environments, and even there some unreactive iron remains after sulfide formation. Data of Rozanov, Volkov, and Yagodinskaya (1974) on Black Sea sediments (see fig. 2) clearly show that sulfide iron rarely exceeds even 50 percent of *reactive* iron, and only when sediments contain extreme sulfur concentrations (>2 wt percent). These data also indicate, as discussed extensively by Berner and Raiswell (1983) that the most sulfur-rich sediments also contain high organic carbon contents as required by the widely accepted Berner (1970, 1984) model for the

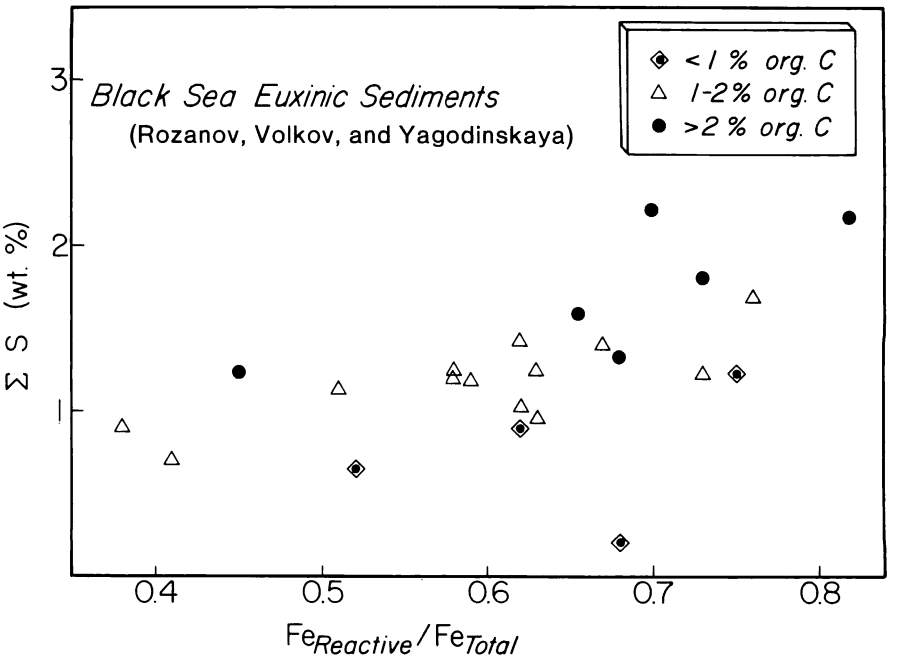

Fig. 2. Plot of total weight percent S against reactive Fe as a fraction of total Fe, based on data for Black Sea euxinic sediments reported by Rozanov, Volkov, and Yagodinskaya (1974). Reactive Fe consists of all Fe that is contained in authigenic minerals (hydroxides, carbonates, silicates, and sulfides) and that can be removed from the sediment using dilute HCl (except for Fe in pyrite which is not soluble but is considered as reactive). Note that for any given Fe(Reactive)/Fe(Total), higher total S contents were found in samples richer in organic carbon, and that the most sulfur-enriched sediments still contained a significant portion of total iron in non-authigenic, detrital minerals.

formation of sedimentary pyrite. In our succeeding discussion, therefore, particularly on the metamorphism of sulfidic marine shales, we will use the assumption that *some* non-sulfide iron was present before metamorphism, except perhaps in the most extreme sulfur-enriched rocks.

The bulk chemical effects of diagenetic sulfidation of detrital material through the Berner (1970) mechanism are illustrated in figure 3 in a simplified chemographic view of a sediment in which sulfur

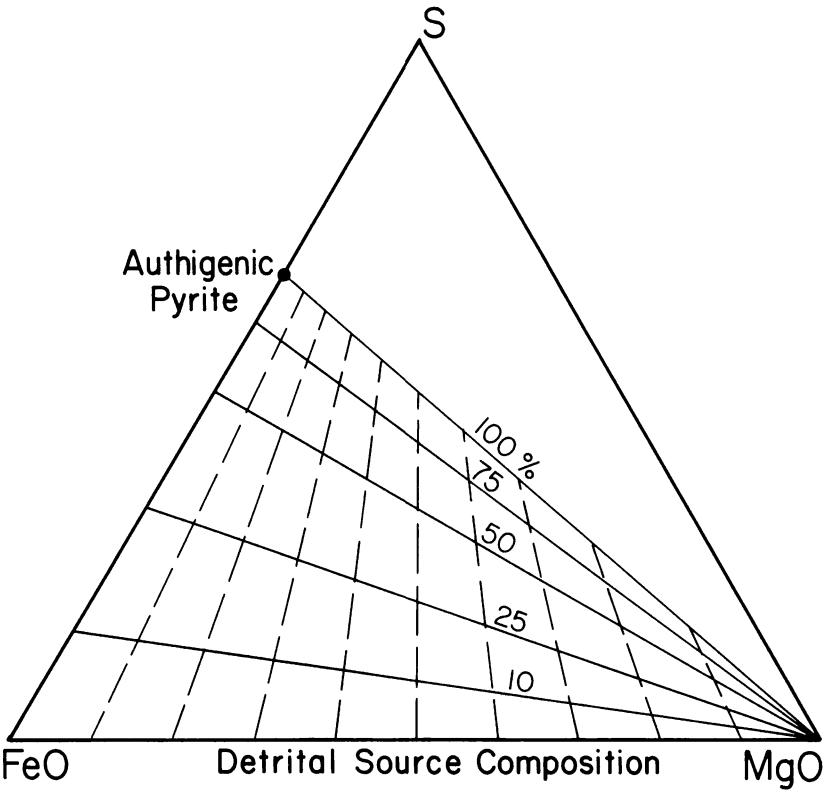

Fig. 3. Diagram of Fe–Mg–S system (atom percent, with excess H_2 and O_2), illustrating diagenetic sulfidation of detrital minerals through reaction with H_2S to produce pyrite plus Mg-enriched detrital compositions. Dashed lines radial from S represent 10 percent progressions in Fe/(Fe + Mg) and are reaction paths for diagenetic sulfidation of detrital minerals. The solid lines indicate progressively greater proportion of total ferromagnesian detrital mineral content that has reacted with H_2S to form authigenic pyrite. Pre-sulfidation bulk compositions lie on the base of the triangle, whereas diagenetic bulk compositions lie at the intersections of the lines radial from S [indicating *original* Fe/(Fe + Mg)] with the lines radial from Mg [indicating the fraction of detrital ferromagnesian minerals sulfidized]. Note that the bulk ratio Fe/(Fe + Mg) of diagenetic material after sulfidation may be predicted by drawing a straight line from pyrite (Py) through the *new* bulk composition to the base of the triangle, and that this value is always lower than that of original detrital material.

variably reacts with detrital minerals. The bulk Fe/(Fe + Mg) (Fe#) of detrital minerals can be represented by a point on the base of the triangle. Dashed lines represent lines radial from S at 10 percent intervals of Fe#. Reaction of sulfur, probably in the form of H_2S (Berner, 1970), with detrital grains will move the sedimentary bulk composition up the appropriate radial line. Note that iron oxide reacting with sulfide will liberate oxygen which can be assumed either to oxidize some organic material or to leave the sediment. The lines labelled 10, 25, 50, and 75 represent percentage molar amounts of reactive ferromagnesian detrital material which has reacted with H_2S, and the points where these lines cross the radial lines show post-diagenetic bulk compositions. A tie-line from pyrite through any of these bulk compositions would indicate the bulk Fe# of post-diagenetic ferromagnesian minerals where it intersects with the base of the triangle. This "new" Fe# may be used to define an effective bulk composition (EBC) of the rock which excludes any iron that is tied up in a reservoir of sulfide, and which is applicable to determination of metamorphic phase equilibria.

It is apparent from figure 3 that for typical intermediate detrital compositions, large extents of diagenetic sulfidation may produce quite magnesian EBC's. This point is critical for the discussion of metamorphic phase equilibria that will follow. Furthermore, a wide range of EBC's may be produced by a combination of variability of original detrital composition and extent of diagenetic sulfidation, as illustrated by figure 4. In this figure, the filled circles indicate 25, 50, and 75 percent sulfidation of original ferromagnesian detrital material with bulk Fe#'s of 0.25, 0.50, and 0.75, as taken from figure 3. The tie-lines shown in figure 4 indicate metamorphic phase relations for (Fe, Mg)silicate–sulfide–oxide assemblages under lower grade (fig. 4A) or higher grade (fig. 4B) metamorphic conditions. As will be discussed below, the progression from higher to lower Fe# in metamorphic minerals is consistent with increasing grade of metamorphism, as well as with sulfidation of silicates. Note that at the metamorphic grade represented by figure 4A, four sulfidized rock compositions contain pyrite only, three contain pyrite plus pyrrhotite (they are therefore on the "pyrrhotite isograd"), and only two contain pyrrhotite alone. At the grade represented by figure 4B, however, there are no rocks with pyrite alone, most bulk compositions have pyrrhotite only, and three of the most sulfidized compositions have pyrite plus pyrrhotite. Most importantly, note that pyrite *cannot be reactively lost* in these compositions under isochemical conditions and will persist until it ultimately melts at temperatures above 700°C (Toulmin and Barton, 1964).

Stable isotopic analyses of sulfur in sulfides from a number of the Massachusetts rocks (Tracy and Rye, 1981) support the assumption that the sulfur in these rocks originated through bacterial reduction of pore-water sulfate under anoxic and possibly euxinic conditions (Berner, 1970). The isotopic data, given in table 4, indicate a range in $\delta^{34}S$

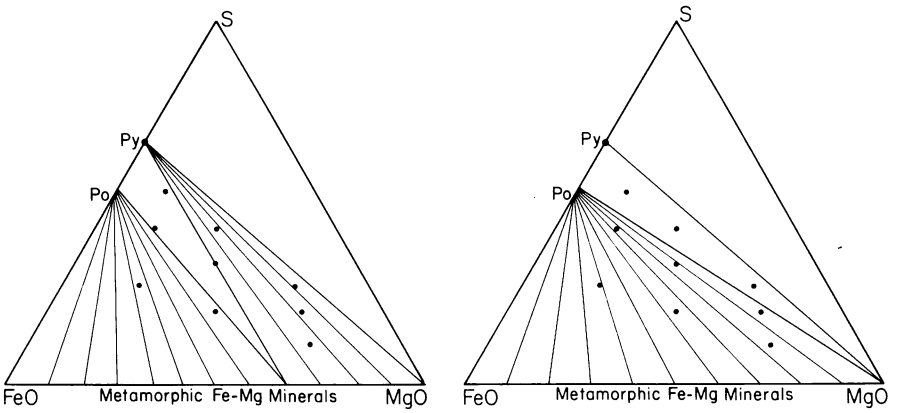

Fig. 4. Fe-Mg-S ternary system similar to figure 3 but now illustrating phase relations for higher-grade metamorphic conditions. Compositions along the base of the triangle are those of the bulk ferromagnesian metamorphic minerals, typically some combination of biotite, chlorite, garnet, cordierite, and ilmenite at lower grade (up to about 525°C) and of biotite, garnet, cordierite, and ilmenite at higher grade (above 525°C). The tielines connect sulfides with bulk ferromagnesian metamorphic mineral composition. The lower apex of the three-phase triangle is the average composition of metamorphic minerals which coexist with both pyrite and pyrrhotite in the assemblage that represents the reaction at the so-called "pyrrhotite isograd." This three-phase triangle will generally sweep from the more iron-rich side of the diagram toward the more magnesian side with increasing metamorphic grade, dehydration, and metamorphic sulfidation (see reaction 6 in the text), as illustrated in the progression from (A) (lower grade) to (B) (higher grade). Filled circles in the figure indicate diagenetic bulk compositions (from fig. 3) produced by 25, 50, and 75 percent diagenetic sulfidation of detrital material with original Fe/(Fe + Mg) of 0.75, 0.50, and 0.25. Note in (B) that some bulk compositions very rich in sulfur cannot lose pyrite from the assemblage through any amount of reaction with silicates and oxides.

TABLE 4

Sulfur isotopic data

Sample	Sulfide assemblage	$\delta^{34}S$ (permil)
FW-882Y	Py + Po	−27.9 (po)
		−29.0 (py)
FW-882E	Py + Po	−27.3 (py)
T-1F	Py + Po	−27.3 (po)
		−27.3 (py)
WN-2B	Po	−25.6 (po)
283	Po	−12.1 (po)

Isotopic data collected by D.M. Rye at Department of Geology and Geophysics, Yale University. $\delta^{34}S$ values of sulfides were determined on SO_2 gas extracted from combustion of mechanically separated pyrite and pyrrhotite. Isotopic analyses of SO_2 gases were performed using a Nuclide 6-60 ratio mass spectrometer, with results reported as permil deviations relative to Cañon Diablo troilite.

from −25 to −30 permil. These very light isotopic compositions are typical of bacterially-reduced sulfur and furthermore suggest that sedimentation rates were low to have allowed this large a sulfate-sulfide fractionation to have occurred (Ohmoto and Rye, 1979). The occurrence of highly sulfidic metamorphosed shales in a belt from Massachusetts north to central Maine in the Middle Silurian stratigraphic level suggests the existence at that time of regions of restricted circulation in which anoxic conditions could develop. In contrast, less extreme sulfidic schists and gneisses of about the same age in this terrane show quite different isotopic behavior. Sample 283 (table 4) is a fairly typical garnetiferous schist with trace amounts of pyrrhotite; its sulfur, though isotopically light, is much less extreme than the other samples and perhaps indicates the less efficient bacterial sulfate reduction that would be expected with more normal sedimentation rates (Berner, 1970; Ohmoto and Rye, 1979).

SILICATE-OXIDE-SULFIDE PHASE RELATIONS

In the past twenty years or so, numerous investigators have attempted to characterize the details of silicate-oxide-sulfide phase relations in medium to high-grade metamorphic rocks (Thompson, 1972; Guidotti, Cheney, and Conatore, 1975; Guidotti, Cheney, and Henry, 1976; Robinson and Tracy, 1977; Tso, Gilbert, and Craig, 1979; Ferry, 1981; Mohr and Newton, 1983) and in metamorphosed ore deposits (Froese, 1969; Nesbitt and Essene, 1983). One common feature of these previous studies and the current report is the documentation of unusually to extraordinarily magnesian assemblages due to effective removal of iron from the reactive bulk composition by sequestering it into a sulfide phase. Thompson (1957) noted that the same effect could be accomplished by oxidation.

As discussed above, Ferry (1981) has argued that the iron depletion may occur in the diagenetic stage. If, however, it occurs during metamorphism, as has been argued above for non-calcareous pelites, the two categories of reaction by which this can be accomplished are: (1) the direct reaction of pyrite with ferromagnesian silicate or Fe-Ti oxide to produce pyrrhotite plus Fe-depleted products, for example:

$$\text{Annite} + 3\ FeS_2 = \text{sanidine} + 6\ FeS + H_2O + 1.5\ O_2 \qquad (1)$$

and (2) the reaction of ferromagnesian silicate or Fe-Ti oxides with a sulfur-bearing fluid (in equilibrium with one or two sulfides plus graphite) to produce pyrrhotite plus Fe-depleted products, for example:

$$\text{Annite} + 3\ H_2S = \text{sanidine} + 3\ FeS + 4\ H_2O. \qquad (2)$$

Both reactions may be referred to as sulfidation reactions, because they are net producers of sulfide minerals, that is, there are more moles of sulfide produced than consumed. The result of both reactions is to

deplete the EBC in iron and to increase the pyrrhotite/pyrite ratio, but an obvious and important difference between the two is that (1) can operate only as long as pyrite remains in the assemblage, whereas (2) may continue above the so-called pyrite-pyrrhotite isograd. In two-sulfide rocks, it is unclear how the production of pyrrhotite is to be partitioned between the two mechanisms.

A third mechanism which increases the pyrrhotite/pyrite ratio without directly involving silicates or oxides is the reaction of pyrite with one or more fluid species to form pyrrhotite and H_2S-enriched fluid. Two such possible reactions are:

$$FeS_2 + 0.5\ CH_4 = FeS + H_2S + 0.5\ C \quad (3)$$

$$FeS_2 + H_2O + 0.5\ C = FeS + H_2S + 0.5\ CO_2 \quad (4)$$

Both these reactions produce H_2S which may then participate in mechanism (2) of the preceding paragraph to sulfidize silicates or oxides. Note that these reactions are either consumers or producers of graphite; equal progress of both will have no effect on the modal graphite in the rock. The reactions are neither sulfidation nor desulfidation reactions because there is no net change in molar sulfide.

From a kinetic and mechanistic point of view, it may be considered more likely that sulfidation of silicates or oxides would occur through reaction with a fluid (reaction (2) above) than a pure solid state reaction (reaction (1) above). The total mineralogical change in the rock can then be predicted through the algebraic combination of reaction (2) with either of the H_2S-producing reactions:

$$\text{Annite} + 3\ FeS_2 + 1.5\ CH_4 = \text{sanidine} + 6\ FeS + 4\ H_2O + 1.5\ C \quad (5)$$

$$\text{Annite} + 3\ FeS_2 + 1.5\ C = \text{sanidine} + 6\ FeS + H_2O + 1.5\ CO_2 \quad (6)$$

where (5) is the combination of (2) and (3), and (6) is the combination of (2) and (4). Note that in both cases the sulfidation of the biotite is accompanied by oxidation of a carbon-bearing species, but of course the oxidation of CH_4 precipitates graphite and increases it modally, whereas the oxidation of graphite through (6) reduces its modal amount. The abundance of graphite in the Massachusetts schists might therefore be taken as evidence for operation of reaction (5) rather than (6).

Experimental data on the sulfidation of synthetic biotites of varying composition were presented by Tso, Gilbert, and Craig (1979). They found that biotites equilibrated to more magnesian compositions in experiments characterized by higher f_{S_2} and contained more S-rich pyrrhotites. Unfortunately, their experimental data are not quantitatively relevant to the present problem for several reasons. They worked at considerably lower P (2 kb), their biotite compositions were more Fe-rich (Fe#'s of 0.496–0.585), and they worked at f_{S_2} values well below those of the pyrite-pyrrhotite equilibrium. Most importantly, they did

not saturate their experimental charges with graphite, so that their fluids were H–O–S rather than C–H–O–S fluids.

It is also important to note that reactions (5) and (3) tend to enrich the fluid in H_2O and H_2S and deplete it in CH_4. X_{CO_2} should not change in the absence of significant oxidation of graphite. Further enrichment of H_2O might occur through the reaction

$$FeTiO_3 + H_2S = TiO_2 + FeS + H_2O \quad (7)$$

which is consistent with mineral assemblages and may be postulated to have gone to completion in the rutile-bearing samples.

Other reactions that have occurred in the sulfidic schists are reflected in the compositions of coexisting silicates, notably biotite, cordierite, and Fe-Ti oxides. Figure 5 illustrates the overall phase equilibria involving sulfides, silicates, and oxides within the tetrahedral four-component representation of the system FeO–MgO–TiO_2–S, projected from graphite, quartz, K-feldspar, and water. In this diagram, biotite has been chosen to represent the bulk ferromagnesian silicate. Assemblage subvolumes within the tetrahedron (including the excess phases graphite, quartz, K-feldspar, cordierite, and fluid) are: (1) the divariant 3-phase assemblage biotite–pyrrhotite–ilmenite; (2) the univariant 4-phase assemblage biotite–pyrrhotite–ilmenite–rutile; (3) the divariant assemblage biotite–pyrrhotite–rutile; (4) the univariant 4-phase assemblage biotite–pyrrhotite–pyrite–rutile; and (5) the divariant 3-phase assemblage biotite–pyrite–rutile. Note that ilmenite and pyrite cannot coexist, and that (5) may be either a volume or reduced to a plane in cases of extreme silicate Mg-enrichment through sulfidation.

The details of the phase equilibria involving silicates are shown in figure 6, a quartz-, K-feldspar- and H_2O-projected AFM diagram (Barker, 1962). Three distinct assemblages which occur at this approximate metamorphic grade (675–720°C, 6 kb) are plotted: garnet–biotite–sillimanite, garnet–cordierite–biotite–sillimanite, and cordierite–biotite–sillimanite. All assemblages contain one or two Fe-Ti oxides, one or two Fe-sulfides, and graphite. Figure 6 emphasizes the large compositional range of biotite and cordierite in the assemblage biotite–cordierite–sillimanite and also shows the distribution of accessory phases which is consistent with the topology shown in figure 5. Dashed lines have been used in figure 6 to indicate the assemblages that are not strictly comparable in metamorphic grade to the ones shown in solid lines. Of the sulfidic schists, T-1F occurs in zone IV and 713 in zone V. The garnet-bearing assemblages shown by dashes are from zones IV and V.

The data portrayed on figure 6 raise the problem of why the biotite–cordierite–sillimanite three-phase triangles should cover such a wide compositional spread when the samples were collected from a small area and all apparently equilibrated under similar conditions of T and P.

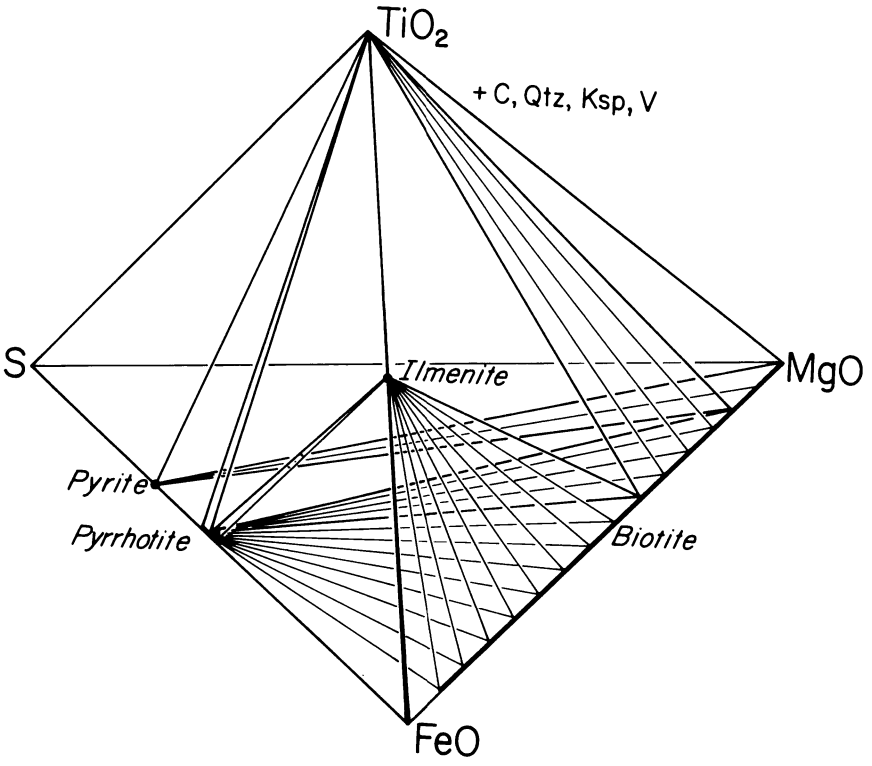

Fig. 5. Illustration of high-grade metamorphic phase relations in the system FeO–MgO–TiO_2–S projected from graphite, quartz, K-feldspar, and H_2O. Note that the base of the tetrahedron is the same system shown in figure 4. Because the system is projected from K-feldspar and quartz, biotite plots along the FeO–MgO join and can be taken as a model of the phase relations of any ferromagnesian silicate. Topology of the diagram is appropriate for f_{O_2}–f_{S_2} conditions precluding stability of magnetite or sulfate. There are five subvolumes within the projected system which represent possible stable assemblages: (1) biotite–ilmenite–pyrrhotite, (2) biotite–ilmenite–rutile–pyrrhotite, (3) biotite–rutile–pyrrhotite, (4) biotite–rutile–pyrrhotite–pyrite, and (5) biotite–rutile–pyrite. Under any given set of fixed intensive parameters, biotite composition is specified for assemblages (2) and (4) and variable in the others. Note that with extreme metamorphic sulfidation and dehydration, the four-phase volume represented by (3) will have a biotite apex at MgO, and subvolume (4) will be reduced to a plane.

The biotite-cordierite-sillimanite three-phase triangle represents the equilibrium

$$4 \text{ biotite} + 8 \text{ sillimanite} + 9 \text{ quartz} = 5 \text{ cordierite} + 4 \text{ K-feldspar} + 1.5\ H_2O \quad (8)$$

coupled with the exchange component $MgFe_{-1}$. Biotite is taken as lying in the eastonite-siderophyllite join, and cordierite is assumed to have 0.5 H_2O per formula unit. This latter value is somewhat arbitrary but is

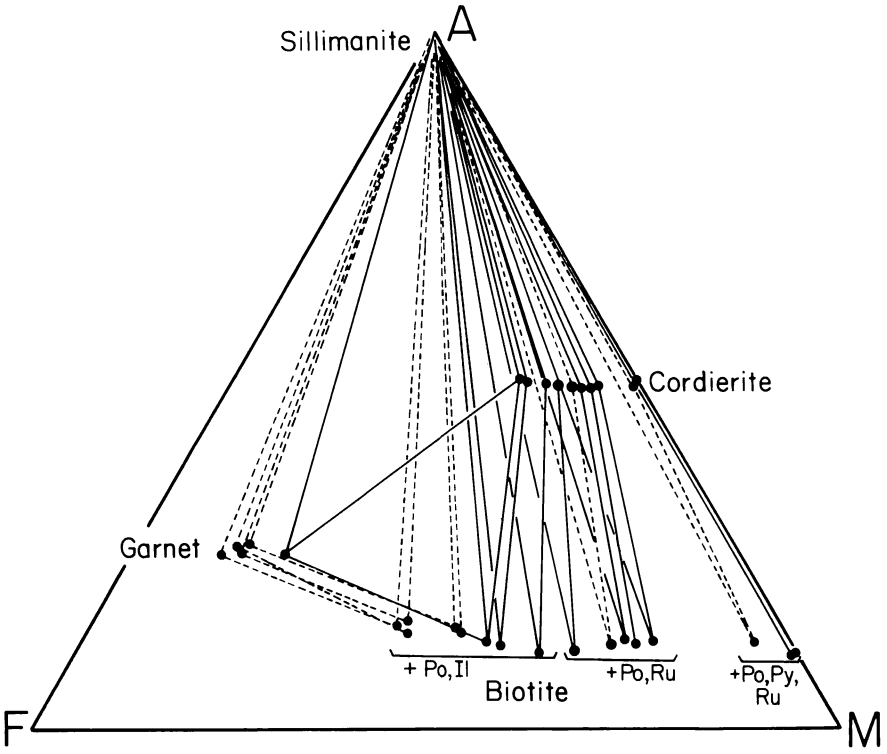

Fig. 6. AFM (Ksp) projection showing the data from tables 2 and 3, along with garnet and biotite data presented elsewhere (Tracy, Robinson, and Thompson, 1976). All assemblages indicated with solid lines are from metamorphic zone VI and formed under very similar conditions of T and P. Assemblages shown using dashed lines are from zones IV and V and formed at temperatures up to 50°C lower than the other samples. Note that accessory minerals occurring in each assemblage type are indicated and correspond with phase relations shown in figure 5.

consistent with cordierite data discussed by Holdaway and Lee (1977). As shown by Thompson (1976), this reaction has a negative dX_{Mg}/dT, indicating that $T_{Fe} > T_{Mg}$, and occurs only in relatively magnesian compositions. The counterpart to (8) for more iron-rich compositions is

6 biotite + 2 sillimanite + 16 quartz

$$= 5 \text{ garnet} + 6 \text{ K-feldspar} + 6\ H_2O \quad (9)$$

which has a positive dX_{Mg}/dT ($T_{Fe} < T_{Mg}$) and which intersects (8) to form the pseudo-univariant reaction (Thompson, 1976:

2 biotite + 2 sillimanite + 9 quartz

$$= \text{garnet} + \text{cordierite} + \text{K-feldspar} + 1.5\ H_2O. \quad (10)$$

All three of the above reactions (8, 9, and 10) are water-producing reactions and therefore their P-T locations will be sensitive to μ_{H_2O} or to a_{H_2O} in metamorphic fluid. Rumble (1974, 1976) has discussed a method of graphically and quantitatively dealing with the effect of variable μ_{H_2O} which is shown in figure 7, a multiple projection from SiO_2, K-feldspar, and sillimanite onto the FMH plane in the system KFMASH. This diagram, which explicitly shows H_2O as a component, rationalizes the overlapping biotite–cordierite–sillimanite three-phase triangles in figure 6 as possibly resulting from variable μ_{H_2O} at approximately constant P and T. In other words, the three-phase triangles are actually three-phase *tie-planes* in the projected three-dimensional composition space AFMH. As clearly indicated in figure 7, the more Mg-rich assemblages comprise tie-planes closer to the H_2O apex and therefore reflect progressively higher μ_{H_2O}.

We can go further in characterizing the μ_{H_2O} variation among the biotite–cordierite–sillimanite assemblages by quantitatively calculating $\Delta\mu_{H_2O}$ using the Gibbs' Method as described by Rumble (1976) and Spear, Ferry, and Rumble (1982). Certain assumptions have been made in setting up the system of equations, notably that the mineral and reaction stoichiometries are as given for eqs (8), (9), and (10) above, and the matrices for assemblages biotite–garnet–sillimanite, biotite–cordierite–sillimanite, and biotite–garnet–cordierite–sillimanite were solved for $\partial\mu_{H_2O}/\partial X_{Mg_{bio}}$. Calculations were done for 700°C and 6 kb,

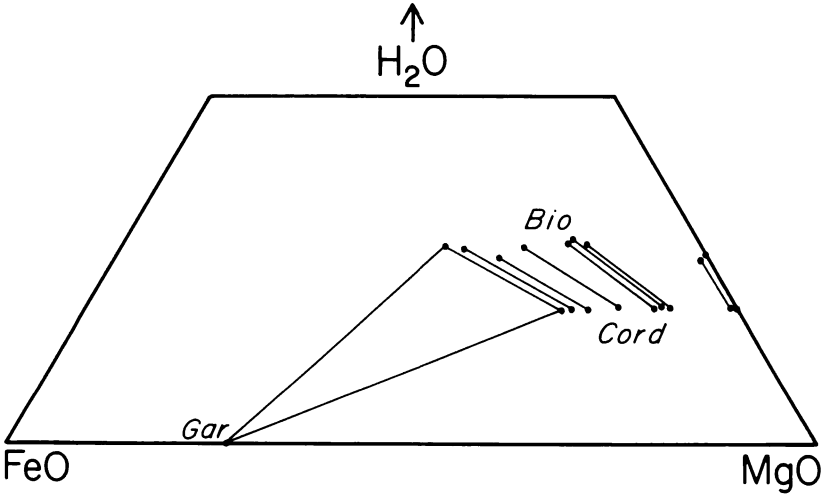

Fig. 7. Projection onto the FMH plane from sillimanite, Kfeldspar and quartz in the system KFMASH (after Rumble, 1974). All sillimanite-bearing assemblages shown in solid lines in Fig. 6 are shown here projected to illustrate that the crossing tielines in the three-phase and four-phase assemblages from Zone VI can be explained by local variations in μ_{H_2O}, with lowest μ_{H_2O} in the garnet-bearing sample 283, and the highest in the Mg-rich, two-sulfide assemblages.

and Fe-Mg K_D's for the various mineral pairs were taken from the compositional data on the four-phase pseudo-univariant assemblage. $\partial\mu_{H_2O}/\partial X_{Mg_{bio}}$ were then integrated over the appropriate composition range for each assemblage to produce the curves shown in figure 8, on which the actual mineral pairs from tables 2 and 3 are plotted. Because we solved for $\Delta\mu_{H_2O}/\Delta X_{Mg_{bio}}$, only the biotite points are constrained to fall on the calculated curves. The closeness of the cordierite points to the calculated curve is, in a sense, a measure of the quality of our calculations. We have not attempted to fix absolute values for μ_{H_2O}, in part because of the assumptions and simplifications we have made in mineral stoichiometry (particularly the assumption of 0.5 H_2O pfu for cordierite), but also because there does not appear to be any relevant appropriate experimental data in the P-T range of interest for the phases of interest. We feel, however, that the assumptions and simplifications we have made will not greatly affect the magnitude of the calculated $\Delta\mu_{H_2O}$ values, particularly within each assemblage type.

We can make some useful inferences from the calculations shown in figure 8. The $\Delta\mu_{H_2O}$-X_{Mg} variations within the biotite–cordierite–sillimanite assemblage are consistent with predictions of T-XMg from Thompson (1976), that is, the most Mg-rich assemblages reflect lower T or higher μ_{H_2O} than more Fe-rich assemblages. There is a rather large

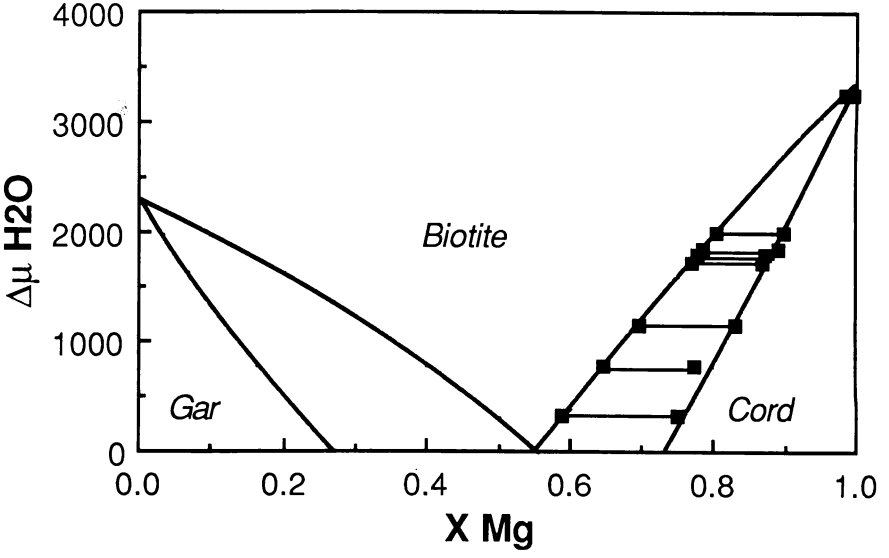

Fig. 8. $\Delta\mu_{H_2O}$–X_{Mg} relations calculated for the multivariant assemblages biotite–cordierite–sillimanite and biotite–garnet–sillimanite using the Gibbs' Method (Spear, Ferry, and Rumble, 1982). Calculations were done as described in the text. Actual compositional data for biotites and cordierites of this study (tables 2 and 3) are plotted to show the consistency of the calculations for the biotite–cordierite–sillimanite loop.

$\Delta\mu_{H_2O}$ of about 3000 cal/mole between the most extreme compositions within the biotite–cordierite–sillimanite assemblage. If we had used a less hydrous cordierite for the calculations, the total $\Delta\mu_{H_2O}$ would have been larger. This large $\Delta\mu$, along with a qualitative estimate of reaction progress based on modal mineralogy, suggests that each sample had its own intrinsic fluid composition, perhaps internally buffered, and that very little external fluid could have been added. Significant volumes of external fluid with water-rich composition would be expected to have overwhelmed the relatively small buffer capacity of the sulfidic assemblages and wiped out any preservation of the fine-scale compositional differences seen in figures 6, 7, and 8.

This dependence of biotite and cordierite compositions on relative values of μ_{H_2O} can be correlated with earlier discussion of the effects of sulfidation on fluid compositions to produce a model for fluid behavior in the sulfidic rocks. Reactions (5) and (7), and possible excess reaction (3) beyond its algebraic contribution to (6), tend to enrich any localized fluid in H_2O, and to a lesser extent in H_2S. We should therefore expect that the greater the degree of sulfidation in a particular sample, the richer the local fluid should be in H_2O. Because the samples with progressively Mg-richer silicates have undergone more sulfidation, it is reasonable to expect that the higher μ_{H_2O} in these samples has stabilized the Mg-richer biotite-cordierite pairs. Stated in another way, the less magnesian biotite-cordierite pairs and the biotite–garnet–cordierite assemblages represent arrested sulfidation—the exhaustion of pyrite in these samples occurred relatively earlier in the metamorphism. After pyrite was gone, sulfidation could not further affect the fluid composition. On the other hand, the samples that retained pyrite at the peak of metamorphism (882E and Y, in particular) would have had the most H_2O (and H_2S) produced, and we should expect the silicate assemblages in these samples to reflect the highest μ_{H_2O}.

Based on these premises, we may postulate not only that external aqueous fluid was unlikely to have been added, but that the internally generated fluid composition did not change after the silicate sulfidation reaction ceased. Alternatively, the mineral assemblage and compositions may have been frozen in at the time that sulfidation ceased, and any ambient fluid then left the rock. In any case, for a suite of samples that all equilibrated at the same T and P, those with the most sulfidized primary compositions clearly document the highest μ_{H_2O}. In earlier published preliminary interpretations of our data (Robinson and Tracy, 1977; Robinson and others, 1982; Robinson and others, 1986), we suggested that in the biotite sulfidation reaction graphite was oxidized according to reaction (6), and the CO_2 produced in this process diluted H_2O in the fluid and lowered μ_{H_2O}. We are no longer confident in this older interpretation, largely due to our more recent estimates that the fO_2 was too low in these rocks to allow significant CO_2 in the fluids (see the discussion of fluid compositions below).

FLUID COMPOSITIONS

Guidotti (1970), Ferry (1981), Mohr and Newton (1983), and Nesbitt and Essene (1983) have calculated fluid compositions containing H_2S from trace amounts to about 10 mole percent for sulfur-rich, graphitic metamorphic environments. Similar calculations for the Massachusetts sulfidic schists show a similar range of fluid compositions for pyrrhotite schists, but much higher H_2S in pyrite-pyrrhotite rocks.

Calculation of fluid compositions was done using general procedures described by Eugster and Skippen (1967), and the assumption of $P_f = P_{tot} = 6000$ bars, $T = 700\,^\circ C$, and ideal mixing of components in the fluid. Thermodynamic data for fluid species were taken from Stull and Prophet (1971), and fugacity coefficients from Ryzhenko and Volkov (1971). Necessary constraints for the calculations are a knowledge of f_{O_2} and f_{S_2}. In the pyrite + pyrrhotite assemblages f_{S_2} is fixed and may be calculated from data of Toulmin and Barton (1964): at 700 °C and 6 kb, $\log f_{S_2} = 0.4$; lower f_{S_2} would apply for pyrrhotite-only assemblages. Establishing f_{O_2} presents more of a problem in the absence of any readily calculated oxygen barometer. Likely maximum values of f_{O_2} can be established from calculations using equations of Ohmoto and Kerrick (1977), which indicate that the upper limit of graphite stability at 700 °C and 6 kb is $\log f_{O_2} = -16.7$ and that the H_2O maximum is at $\log f_{O_2} = -17.8$ (see fig. 9).

In order to provide a closer constraint on f_{O_2}, the $\log f_{O_2}$–$\log f_{S_2}$ diagram shown in figure 9 was calculated. Construction of the diagram was done according to the suggestions of Froese (1977) using thermodynamic data from Robie and others (1978) and Toulmin and Barton (1964) to construct the sulfide and oxide field boundaries. Also shown in figure 9 are stability curves for the sulfidation reaction of two biotite compositions, Fe# = 0.33 and Fe# = 0.01. The first was chosen because this is the approximate biotite composition that lies at the ilmenite-rutile "fence" on the AFM diagram (see fig. 6), and its intersection with the ilmenite-rutile boundary in $\log f_{O_2}$–$\log f_{S_2}$ space should fix both f_{O_2} and f_{S_2} for this bulk composition. The second biotite is that which occurs in a two-sulfide rock (882Y), and therefore the intersection of its stability curve with the pyrite-pyrrhotite boundary should fix f_{O_2} and f_{S_2} in this sample.

The biotite stability curves were calculated in the same manner as Froese (1977) caculated the f_{O_2}–f_{S_2} stability of grunerite and as Tso, Gilbert, and Craig (1979) constructed biotite stability curves. Like these authors, we used an ideal solution model for the hydrous silicate to calculate activities, and we used annite-phlogopite stoichiometry. The sulfidation reaction used was

$$\text{Annite} + 1.5\ S_2 = \text{sanidine} + 3\ FeS + H_2O + 1.5\ O_2 \qquad (11)$$

The value of ΔG_f° for annite was taken from Zen (1985) and other thermochemical data from Robie, Hemingway, and Fisher (1978). Note

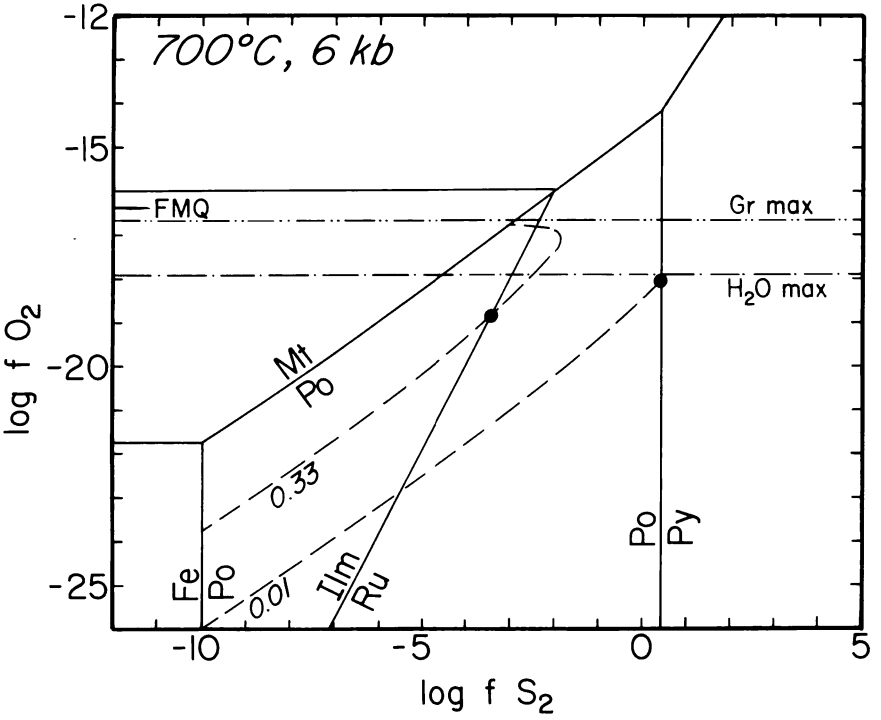

Fig. 9. Log f_{O_2}–log f_{S_2} diagram calculated for 700°C and 6 kb, as described in the text. Boundaries for Fe-oxide and Fe-sulfide mineral fields are shown, along with the positions of maximum f_{O_2} of graphite stability and of the H_2O maximum (Ohmoto and Kerrick, 1977). Dashed curves are calculated stabilities of biotite occurring in an assemblage with ilmenite + rutile (labelled 0.33) and of biotite occurring with pyrite + pyrrhotite (labelled 0.01). Pronounced curvature of these calculated stability curves is due to variations in compositions of graphite-saturated fluids, in particular X_{H_2O}. Filled circles denote f_{O_2} and f_{S_2} conditions specified by these two biotite compositions.

that the biotite stability boundaries in figure 9 are curved, whereas those shown for (Fe, Mg)-grunerite in Froese (1977) and for biotite in Tso, Gilbert, and Craig (1979) were straight. The reason for this is that these other authors calculated stability of a hydrous ferromagnesian silicate in f_{O_2}–f_{S_2} space without any graphite present, and therefore there was no significant variation in water content of the fluid. On the graphite-saturated f_{O_2}–f_{S_2} diagram of figure 9, however, there is substantial variation in proportions of C–O–H–S fluid species which will obviously affect the stability of hydrous phases. This phenomenon is especially apparent in the stability curve for Fe# = 0.33 at f_{O_2} above the water-maximum in figure 9. The very rapid decline in X_{H_2O} in this f_{O_2} range (Ohmoto and Kerrick, 1977) dramatically reduces the f_{S_2} stability of iron-bearing biotite.

Theoretically, the composition of pyrrhotite (N_{FeS}) itself should fix f_{S_2} for any pyrite-absent sample (Toulmin and Barton, 1964), and this f_{S_2}, along with a calculated biotite stability curve for that sample, should fix the f_{O_2} and f_{S_2}. Practically, however, it is difficult to determine with confidence the composition of pyrrhotites, because this phase readily reequilibrates down to very low T during cooling (Craig and Scott, 1974). Microprobe analyses of pyrrhotites in single samples showed great enough scatter to induce caution.

Using the f_{O_2} and f_{S_2} constraints taken from figure 9, fluid compositions for samples 882E (nearly pure Mg-biotite) and WN-1A (closest sample to the Fe# of the rutile-ilmenite "fence") were calculated and are presented in table 5. There is obviously some uncertainty in these calculated fluid compositions, the largest source of error being error in estimation of actual values for f_{O_2} in sample 882E and f_{O_2} and f_{S_2} in WN-1A due to error in the thermodynamic calculation of biotite stability in the sulfidation reaction. In turn, principal sources of error in this calculation are errors in values of $\Delta G_f°$ for annite and other phases in reaction (11), in the assumption of ideal solid solution in biotite in estimating a_{annite} for very dilute annite-phlogopite solid solutions, and in modelling natural, compositionally complex biotites as ideal annite-phlogopite. We estimate that error from these sources will not greatly affect our conclusions.

The fluid compositions given in table 5 are rather interesting, in particular the very high X_{H_2S} in 882E. This high value is consistent with a model discussed above for hydrolysis of pyrite to produce H_2S and pyrrhotite, and the resulting high f_{H_2S} would have driven sulfidation reactions like (5) and (7) to produce near-total removal of iron from silicates and oxides, and therefore from the EBC. It is also consistent with the occurrence of H_2S in Mg-cordierite. It is also notable that CO_2 is the dominant carbon-bearing species despite the low f_{O_2} below the water-maximum, which typically results in CH_4-H_2O fluids (Ohmoto and Kerrick, 1977). The difference in this case is caused by the unusually high sulfur fugacity which allows replacement of CH_4 by H_2S as the reduced species in the fluid. Calculations show that at this f_{S_2}, but at lower f_{O_2} ($<10^{-18}$), the fluid becomes an almost binary H_2S-H_2O fluid that approaches pure H_2S at f_{O_2} below 10^{-20}.

The fluids in one-sulfide rocks such as WN-1A are obviously going to be much poorer in H_2S, as shown by table 5. In fact, the calculations

TABLE 5

Calculated fluid compositions at 700°C, 6000 bars

Sample	Log f_{O_2}	Log f_{S_2}	H_2O	H_2S	X_i CO_2	CH_4	H_2
FW882E	−17.8	+0.4	0.353	0.506	0.130	0.009	0.002
WN-1A	−18.3	−3.5	0.794	0.036	0.051	0.113	0.006

show that they become water-dominant, but this result is puzzling in light of the discussion in the previous section of higher μ_{H_2O} in the more Mg-rich sulfidic assemblages containing biotite and cordierite. We cannot explain this enigma at this time, but further research on the fluids in the sulfidic rocks, both calculations and fluid inclusion observations, is currently underway.

SUMMARY

Study of unusually sulfidic and graphitic pelitic schist samples from central Massachusetts indicates that these samples were metamorphosed at temperatures ranging from 650°C (metamorphic zone IV) to 725°C (metamorphic zone VI). A majority of them, however, equilibrated at about the same temperature and pressure (700°C, 6 kb). Both major element and sulfur isotopic chemistry of these rocks suggest that the protoliths formed under anoxic, and perhaps euxinic, conditions. The variety of mineral assemblages and compositions in these rocks document variation in f_{O_2}, f_{S_2}, and μ_{H_2O}, all of which can be ascribed to inherited variation in protolith chemistry. Pyrrhotite-bearing schists contain the assemblages garnet–cordierite–biotite–sillimanite–ilmenite, cordierite–biotite–sillimanite–ilmenite, and cordierite–biotite–sillimanite–rutile (all with quartz, plagioclase, K-feldspar, and graphite), with progressively more magnesian biotite and cordierite. Schists with both pyrite and pyrrhotite contain essentially pure magnesian cordierite and biotite, along with sillimanite, graphite, quartz, rutile, and feldspars.

Our analysis of phase equilibria in these rocks leads us to propose that they were isochemically metamorphosed, and that the more sulfur-rich the sedimentary protoliths were, the more magnesian the resulting metamorphic silicate-oxide assemblage became. It is important to note here that by sulfur-rich we mean a *ratio* of S/Fe approaching 1.0 or greater, rather than any absolute amount of sulfur. The shift in effective bulk composition of all minerals in the rock exclusive of sulfides was accomplished through reaction of one mole of pyrite (FeS_2) to form about two moles of pyrrhotite ($\approx Fe_{.92}S$), with the higher Fe/S ratio in bulk sulfide produced through reduction of ferrous oxide formerly present in silicates or oxides. Therefore, the pyrrhotite-only samples contain the AFM assemblage cordierite–biotite–sillimanite, in which biotite and cordierite have a very wide range in Fe# which reflects variation in the initial ratio of pyrite to ferromagnesian detrital minerals in the protoliths. All these samples crossed the so-called "pyrrhotite isograd" at which pyrite was completely consumed.

The most extreme sulfidic schists, however, were incapable of crossing this isograd because they had such high S/Fe. In these samples (882E and Y, T-1F) there was not enough non-sulfide iron to allow for isochemical transformation of pyrite to pyrrhotite, and thus the ultimate high-grade assemblage retained pyrite, at a metamorphic grade far above its usual stability limit, along with a nearly Fe-absent silicate-oxide

assemblage. We have not been able to constrain closely the AFM boundary between pyrrhotite only and pyrrhotite-pyrite assemblages except to say that it lies at biotite Fe#'s between 0.2 (po only) and about 0.05 (py + po), although at this high grade it is likely to be closer to this latter value.

The stability of the low-variance (pseudo-divariant) AFM assemblage cordierite–biotite–sillimanite over a wide range of compositions for samples apparently equilibrated at about the same T and P implies that there was substantial difference in fluid compositions, especially in μ_{H_2O}, between samples. Gibbs' Method calculations in the cordierite–biotite–sillimanite AFM (Kspar) assemblage at 700°C and 6 kb indicate that the most magnesian cordierite–biotite–sillimanite assemblages had a μ_{H_2O} about 3000 calories higher than the most ferrous assemblages. This large a μ_{H_2O} difference was presumably produced through internal fluid buffering accomplished by fluid-producing or fluid-consuming reactions within each sample in which there is effective local control of fluid composition. Because the modal amounts of minerals that can affect fluid compositions are small, and thus the buffer capacities of the rocks are limited, this observation argues against pervasive flow of large volumes of externally-derived fluid.

Fluid composition calculations were attempted for two typical samples, a highly magnesian one containing both pyrite and pyrrhotite, and one near the rutile-ilmenite AFM boundary and containing pyrrhotite only. These calculations required estimates of oxygen and sulfur fugacities as constraints. f_{S_2} was calculated from data of Toulmin and Barton (1964), and f_{O_2} was estimated from calculations based on thermodynamic stability of biotite in the sulfidation reaction. The results of the calculations indicate quite different fluids were likely present in the two samples: an H_2S- and H_2O-dominated fluid (51 mole percent H_2S, 35 mole percent H_2O) in the sulfur-rich sample; an H_2O- and CH_4-rich fluid with more than an order of magnitude less H_2S (<4 mole percent) in the other. The source of greatest uncertainty in calculating these fluids is uncertainty in f_{O_2}, which is not well constrained. Minor variations in f_{O_2} can cause major shifts in calculated fluids. One interesting observation from the calculations is that under these high f_{S_2} conditions, methane is almost entirely replaced by hydrogen sulfide as a reduced species in graphite-saturated fluids, resulting in a nearly binary H_2S-H_2O fluid with very little carbon in it.

ACKNOWLEDGMENTS

The authors thank a number of colleagues who have helped the progress of this investigation or discussed various aspects of it with us, especially R. D. Tucker, M. T. Field, D. M. Rye, D. W. Mohr, J. M. Ferry, and M. P. Dickenson. We especially thank Tucker, Field, and H. N. Berry IV for their assistance in locating and collecting sulfidic schist samples. D. A. Hewitt provided a very helpful review of an earlier version of the manuscript. Financial support has been provided by the

National Science Foundation through grant EAR 83-19673 (to Tracy); through several grants from the Geology and Geochemistry Programs to Robinson; through support for sulfur-isotope analysis by National Science Foundation grant EAR-7903769 (to Danny M. Rye and Tracy).

REFERENCES

Albee, A. L., and Ray, L., 1970, Correction factors for electron probe microanalysis of silicates, oxides, carbonates, phosphates and sulfates: Anal. Chemistry, v. 42, p. 1408–1414.

Barker, Fred, 1962, Cordierite-garnet gneiss and associated microcline-rich pegmatite at Sturbridge, Mass. and Union, Conn.: Am. Mineralogist, v. 47, p. 907–918.

Bence, A. E., and Albee, A. L., 1968, Empirical correction factors for the electron microanalysis of silicates and oxides: Jour. Geology, v. 76, p. 382–403.

Berner, R. A., 1970, Sedimentary pyrite formation: Am. Jour. Sci., v. 268, p. 1–23.

———— 1981, A new geochemical classification of sedimentary environments: Jour. Sed. Pet., v. 51, p. 359–365.

———— 1984, Sedimentary pyrite formation: an update: Geochim. et Cosmochim. Acta, v. 48, p. 605–615.

Berner, R. A., and Raiswell, R., 1983, Burial of organic carbon and pyrite sulfur in sediments over Phanerozoic time: a new theory: Geochim. et Cosmochim. Acta, v. 47, p. 855–862.

Craig, J. R., and Scott, S. D., 1974, Sulfide phase equilibria, *in* Ribbe, P. H., ed., Sulfide Mineralogy: Mineralog. Soc. America Short Course Notes, v. 1, p. CS-1-CS-110.

Eugster, H. P., and Skippen, G. B., 1967, Igneous and metamorphic reactions involving gas equilibria, *in* Abelson, P. H., ed., Researches in Geochemistry, v. 2: New York, John Wiley & Sons, p. 492–521.

Ferry, J. M., 1981, Petrology of graphitic sulfide-rich schists from south-central Maine: an example of desulfidation during prograde regional metamorphism: Am. Mineralogist, v. 66, p. 908–931.

Field, M. T., 1975, Bedrock Geology of the Ware Area, Central Massachusetts: Ph.D. thesis, Univ Massachusetts, Amherst, Dept. Geology Geography Contr. 22, 186 p.

Froese, E., 1969, Metamorphic rocks from the Coronation Mine and surrounding area: Canada Geol. Survey Paper 68-5, p. 55–77.

———— 1971, The graphical representation of sulfide-silicate phase equilibria: Econ. Geology, v. 66, p. 335–341.

———— 1977, Oxidation and sulphidation reactions, *in* Greenwood, H. J., ed., Application of thermodynamics to petrology and ore deposits: Mineralog. Assoc. Canada Short Course Notes, v. 2, p. 84–98.

Guidotti, C. V., 1970, The mineralogy and petrology of the transition from the lower to upper sillimanite zone in the Oquossoc area, Maine: Jour. Petrology, v. 11, p. 277–336.

———— 1984, Micas in metamorphic rocks, *in* Bailey, S. W., ed., Micas: Reviews in Mineralogy, v. 13, p. 357–468.

Guidotti, C. V., Cheney, J. T., and Conatore, P. D., 1975, Coexisting cordierite + biotite + chlorite from the Rumford quadrangle, Maine: Geology, v. 3, p. 147–148.

Guidotti, C. V., Cheney, J. T., and Henry, D. J., 1976, Sulfide-silicate phase relations in metapelites of northwestern Maine [abs.]: EOS, v. 58, p. 524.

Guidotti, C. V., Cheney, J. T., and Guggenheim, S., 1977, Distribution of titanium between coexisting muscovite and biotite in pelitic schists from northwestern Maine: Am. Mineralogist, v. 62, p. 438–448.

Hewitt, D. A., and Wones, D. R., 1984, Experimental phase relations of the micas, *in* Bailey, S. W., ed., Micas: Reviews in Mineralogy, v. 13, p. 201–256.

Holdaway, M. J., and Lee, S. M., 1977, Fe-Mg cordierite stability in high-grade pelitic rocks based on experimental, theoretical and natural observations: Contr. Mineralogy Petrology, v. 63, p. 175–198.

Mohr, D. A., and Newton, R. C., 1983, Kyanite-staurolite metamorphism in sulfidic schists of the Anakeesta Formation, Great Smoky Mountains, North Carolina: Am. Jour. Sci., v. 283, p. 97–134.

Munoz, J. L., and Ludington, S. D., 1974, Fluorine-hydroxyl exchange in biotite: Am. Jour. Sci., v. 274, p. 396–413.

Nesbitt, B. E., and Essene, E. J., 1983, Metamorphic volatile equilibria in a portion of the southern Blue Ridge Province: Am. Jour. Sci., v. 283, p. 135–165.

Nesbitt, B. E., and Kelly, W. C., 1980, Metamorphic zonation of sulfides, oxides and graphite in and around the orebodies at Ducktown, Tennessee: Econ. Geology, v. 75, p. 1010–1021.

Ohmoto, H., and Kerrick, D. M., 1977, Devolatilization equilibria in graphitic systems: Am. Jour. Sci., v. 277, p. 1013–1044.

Ohmoto, H., and Rye, R. O., 1979, Isotopes of sulfur and carbon, *in* Barnes, H. L., ed., Geochemistry of Hydrothermal Ore Deposits, 2d ed.: New York: John Wiley & Sons, p. 509–567.

Raiswell, R., and Berner, R. A., 1985, Pyrite formation in euxinic and semieuxinic sediments: Am. Jour. Sci., v. 285, p. 710–724.

Robie, R. A., Hemingway, B. S., and Fisher, J. R., 1978, Thermodynamic Properties of Minerals and Related Substances at 298.15 K and 1 bar (10^5 Pascals) Pressure and at Higher Temperatures. U.S. Geol. Survey Bull. 1452, 456 p.

Robinson, Peter, 1982, Realms of regional metamorphism in southern New England, with emphasis on the eastern Acadian metamorphic high, *in* Schenk, P. E., ed., Regional Trends in the Geology of the Appalachian-Caledonian-Hercynian-Mauritanide Orogen: Boston, D. Reidel, p. 249–258.

Robinson Peter, and Tracy, R. J., 1977, Sulfide-silicate-oxide equilibria in sillimanite-Kfeldspar grade pelitic schists, central Massachusetts [abs.]: EOS, v. 58, p. 524.

Robinson, Peter, Tracy, R. J., Hollocher, K. T., and Dietsch, C. W., 1982, High grade Acadian regional metamorphism in south-central Massachusetts, *in* Joesten, R., and Quarrier, S. S., eds., Guidebook for Fieldtrips in Connecticut and South-Central Massachusetts: Hartford, Connecticut Geol. and Nat. History Survey, Guidebook 5, p. 289–339.

Robinson, Peter, Field, M. T., and Tucker, R. D., 1982, Stratigraphy and structure of the Ware-Barre area, central Massachusetts, *in* Joesten, R., and Quarrier, S. S., eds., Guidebook for Fieldtrips in Connecticut and South-Central Massachusetts: Hartford, Connecticut Geol. and Nat. History Survey, Guidebook 5, p. 341–373.

Robinson, Peter, Tracy, R. J., Hollocher, K. T., Schumacher, J. T., and Berry, H. N. IV, 1986, The central Massachusetts metamorphic high, *in* Robinson, Peter, and Elbert, D. C., eds., Field Trip Guidebook: Regional Metamorphism and Metamorphic Phase Relations in Northwestern and Central New England (Field Trip B-5): Internat. Mineralog. Assoc., 14th General Mtg. Stanford Univ., Contr. 59 (Dept. Geology and Geography, Univ. Massachusetts, Amherst), p. 195–266.

Rosenfeld, J., 1969, Stress effects around quartz inclusions in almandine and the piezothermometry of coexisting aluminum silicates: Am. Jour. Sci., v. 267, p. 317–351.

Rozanov, A. G., Volkov, I. I. and Yagodinskaya, T. A., 1974, Forms of iron in surface layer of Black Sea sediments, *in* Degens, E. T., and Ross, D. A., eds., The Black Sea—Geology, Chemistry and Biology: Am. Assoc. Petroleum Geologists, Mem. 20, p. 532–541.

Rumble, D. III, 1974, Gradients in the chemical potentials of volatile components between sedimentary beds of the Clough Formation, Black Mountain, New Hampshire: Carnegie Inst. Washington Year Book 73, p. 371–380.

———— 1976, The use of mineral solid solutions to measure chemical potential gradients in rocks: Am. Mineralogist, v. 61, p. 1167–1174.

Ryzhenko, B. N., and Volkov, V. P., 1971, Fugacity coefficients of some gases in a broad range of temperatures and pressures: Geochem. Internat., v. 8, p. 468–481.

Spear, F. S., Ferry, J. M., and Rumble, D., III, 1982, Analytical formulation of phase equilibria: the Gibbs' Method, *in* Ferry, J. M., ed., Characterization of Metamorphism through Mineral Equilibria: Review in Mineralogy, v. 10, p. 105–152.

Stull, D. R., and Prophet, H., 1971, JANAF Thermochemical Tables: Washington, D.C. U.S. Dept. Commerce.

Thompson, A. B., 1976, Mineral reactions in pelitic rocks: Am. Jour. Sci., v. 276, p. 401–454.

Thompson, J. B., Jr., 1957, The graphical analysis of mineral assemblages in pelitic schists: Am. Mineralogist, v. 42, p. 842–858.

———— 1972, Oxides and sulfides in regional metamorphism of pelitic schists: Internat. Geol. Cong., 24th, Montreal 1972, sec. 10, p. 27–35.

Toulmin, P., III, and Barton, P. B., Jr., 1964, A thermodynamic study of pyrite and pyrrhotite: Geochim. et Cosmochim. Acta, v. 28, p. 641–671.

Tracy, R. J., 1978, High grade metamorphic reactions and partial melting in pelitic schist, west-central Massachusetts: Am. Jour. Sci., v. 278, p. 150–178.

Tracy, R. J., and Robinson, Peter, 1980, Evolution of metamorphic belts: Information

Tracy, R. J., Robinson, Peter, and Thompson, A. B., 1976, Garnet composition and zoning in the determination of temperature and pressure of metamorphism, central Massachusetts: Am. Mineralogist, v. 61, p. 762–775.

Tracy, R. J., and Rye, D. M., 1981, Origin and mobility of sulfur in graphitic schists, central New England [abs.]: Geol. Soc. America, Abs. with Programs, v. 13, p. 569.

Tso, J. L., Gilbert, M. C., and Craig, J. R., 1979, Sulfidation of synthetic biotites: Am. Mineralogist, v. 64, p. 304–316.

Valley, J. W., Petersen, E. U., Essene, E. J., and Bowman, J. R., 1982, Fluorphlogopite and fluortremolite in Adirondack marbles and calculated C-O-H-F fluid compositions: Am. Mineralogist, v. 67, p. 545–557.

Zen, E-An, 1985, An oxygen buffer for some peraluminous granites and metamorphic rocks: Am. Mineralogist, v. 70, p. 65–73.